ELSEVIER

Journal of Organometallic Chemistry 545–546 (1997) 315–326

Journal of Organometallic Chemistry

^{187}Os, ^{31}P and ^{17}O NMR study of carbonylated and alkylated (*p*-cymene)OsI (L)PR_3 complexes [1]

Andreas Gisler, Martina Schaade, Eric J.M. Meier, Anthony Linden, Wolfgang von Philipsborn *

Organisch-chemisches Institut, Universität Zürich, Winterthurerstr. 190, CH-8057 Zürich, Switzerland

Received 14 March 1997

Abstract

Series of complexes of the types [(*p*-cymene)OsI(CO)PR_3][PF_6], (*p*-cymene)OsI(phenylethynyl)PR_3, (*p*-cymene)OsI(alkyl)PR_3 have been prepared and investigated by ^{187}Os, ^{31}P and ^{17}O NMR spectroscopy. The structures of (*p*-cymene)OsI(C≡CPh)PMe_3 (**3a**) and (*p*-cymene)OsI(C≡CPh)P^{i}Pr$_3$ (**3c**) have been determined by X-ray diffraction. A mechanistic study of the formation of the metallacycle **8A** formed by intramolecular trans-alkylation from (*p*-cymene)OsI_2P^{i}Pr$_3$ (**1c**) in the presence of Al_2Me_6 is presented. As shown by time-dependent ^{31}P NMR, (*p*-cymene)OsI(Me)P^{i}Pr$_3$ (**6c**) is formed as an intermediate. ^{187}Os,^{13}C coupling constants in Cp- and Cp*Os(CO)$_2$Me (**14** and **15**) have been determined from ^{13}C-filtered (^1H,^{187}Os)-HMQC correlation spectra and are interpreted in comparison with the ^{57}Fe,^{13}C data of the corresponding iron complexes. © 1997 Elsevier Science S.A.

1. Introduction

The increasing interest in the chemistry of (organo)osmium complexes [1,2] has led us to investigate the coordination sphere of the transition metal by ^{187}Os NMR. In our first communication [3] we have reported ^{187}Os chemical shifts, ^{187}Os,^{31}P coupling constants, and ^{187}Os spin-lattice relaxation times T_1 of the parent complexes (*p*-cymene)OsX_2L (X = Cl, I; L = PR_3, $P(OR)_3$), and have correlated the osmium shielding data with steric and electronic ligand parameters. Also of particular interest, in relation to comparisons with corresponding iron complexes [4,5], is the investigation of the Os,C bond in carbonylated and alkylated complexes by means of ^{187}Os,^{13}C one-bond spin coupling. In the case of osmium(carbonyl) complexes, the extent of Os,C bonding and back-bonding is also reflected in the ^{17}O NMR shielding data of the carbonyl oxygen atom which have proven readily accessible by high-field ^{17}O NMR at 14.1 Tesla.

(*p*-Cymene)osmium complexes have previously been studied by Cabeza and Maitlis [6], Werner et al. [7], and Knaup and Werner [8]. We have made use of the reported synthetic procedures to prepare series of model complexes of the types [(*p*-cymene)OsI(CO)PR_3][PF_6], (*p*-cymene)OsI(phenylethynyl)PR_3, (*p*-cymene)OsI(alkyl)PR_3, and CpOs(CO)$_2$Me in order to study their ^{187}Os, ^{31}P, ^{17}O and ^{13}C NMR spectra.

Organometallic applications of ^{187}Os NMR spectroscopy are still scarce and have so far been concerned with μ-hydrido binuclear complexes [9–11], a range of $CpOsL_2R$ complexes [12,13], (*p*-cymene)OsX_2L complexes [3], the utilisation of ^{187}Os,^{13}C spin coupling to study osmium carbonyl clusters [14,15] and a study of osmium(diketonate) complexes [16].

2. Results and discussion

2.1. Synthesis

Starting from (*p*-cymene)OsI_2PR_3 (**1a–f**) [3], the preparation of the carbonylated cationic complexes [(*p*-cymene)OsI(CO)PR_3][PF_6] (**2a–f**) was achieved following the procedure that Werner and Zenkert [17] used for the preparation of the trimethylphosphine complex. An analogous method previously described for the introduction of the phenylacetylene ligand in

* Corresponding author.

[1] Transition Metal NMR Spectroscopy Part XXXVII, Part XXXVI [D. Rentsch, R. Hany, W. von Philipsborn, Magn. Reson. Chem., 1997, in press].

PII S0022-328X(97)00376-8

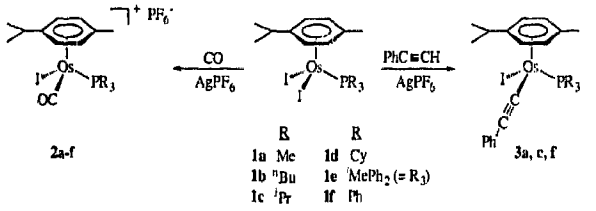

Scheme 1.

(benzene)OsI_2PR_3 complexes [8] also proved applicable in the (*p*-cymene) case and led to complexes **3a**, **3c** and **3f** (Scheme 1). On the other hand, alkylation was shown to be successful in the case of the trimethylphosphine carbonyl complex **2a** [18]. However, in our hands, alkylation of the cationic mono-iodo complexes **2a–f** with a variety of nucleophilic reagents, such as Grignard reagent, alkyllithium or cuprates, was unsuccessful. For this reason, introduction of the alkyl group was attempted with the parent diiodo complexes **1a** and **1c**. From the work of Cabeza and Maitlis [6] on the dichloro complexes, it is known that the type of product from the methylation reaction with Al_2Me_6 depends very much on the ligand L and the reaction conditions. We have observed that the diiodo complex **1a** reacts with $AlEt_3$ to form the desired monoalkyl compound (*p*-cymene)OsI(Et)PMe_3 (**4a**) [19] in 30% yield, whereas the triisopropylphosphine and tricyclohexylphosphine derivatives, **1c** and **1d**, respectively, gave only hydridic products (Scheme 2).

The reaction of the diiodo complexes with Al_2Me_6 was even more complicated. In contrast with the successful ethylation of **1a**, no reaction with Al_2Me_6 took place. The triisopropylphosphine complex **1c** likewise did not yield isolable amounts of the monomethyl derivative, however, upon prolonged treatment with an excess of Al_2Me_6, yielded 35% of a new compound subsequently shown to be the metallacycle **8**. A detailed low-temperature NMR investigation of this reaction (described below) revealed that the expected monomethyl complex is formed exclusively at 228 K and subsequently reacts to give the metallacycle **8** even at low temperature (vide infra). Quenching of a preparative-scale reaction at low temperature gave a mixture of the mono- and dimethyl complexes **6c** and **7c**, respectively (Schemes 3 and 5). The intramolecular cyclisation reaction is not observed with the tricyclohexyl derivative **1d**, presumably for steric reasons, and the expected monomethyl complex **6d** is formed.

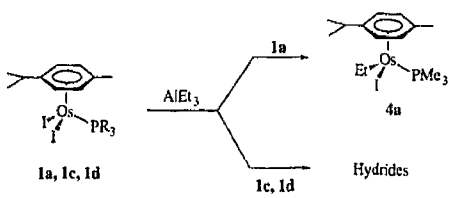

Scheme 2.

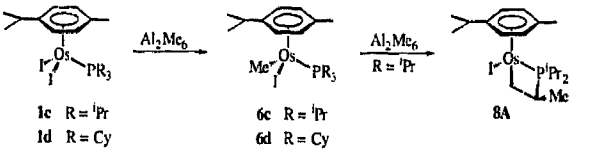

Scheme 3.

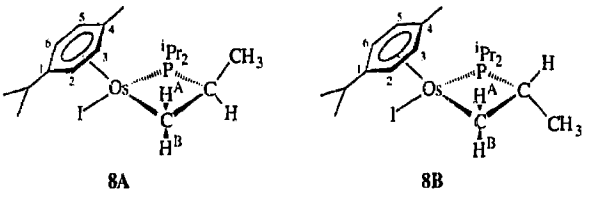

Scheme 4.

2.2. Structure and formation of the metallacycle 8

The yellow-orange solid gives a highly informative ^1H NMR spectrum displaying four well-separated multiplets for the four tertiary CH groups ($CH(CH_3)_2$ of (*p*-cymene) and the three phosphine substituents), which in the ^{31}P decoupled $^1H,^1H$ COSY spectrum, correlate with only seven methyl resonances. The eighth methyl group has now become a methylene group in the cyclic $Os–CH^AH^B–CH(CH_3)–P$ structural unit. This was confirmed by the corresponding $^{13}CH^AH^B$ resonance (−12.8 ppm), which clearly shows that it is a methylene group attached to the metal centre, and by a $^1H,^{187}Os$ correlation experiment. From the complete ^1H and ^{13}C NMR signal assignments (see Section 4), two diastereomeric structures **8A** and **8B** can be postulated (Scheme 4). The two vicinal $^3J(^{31}P,^1H)$ coupling constants for the diastereotopic methylene protons (36.4 and 4.6 Hz) are in agreement with the H–C–C–P torsional angles observed in a Dreiding model for a puckered conformation of the four-membered ring with a quasi-axial H^A. A NOESY experiment further revealed that only H^A (1.62 ppm, $^3J(^{31}P,^1H) = 4.6$ Hz) exhibits a cross peak with the arene protons at C(2) and C(5). The diastereomeric structures **8A** and **8B** can be

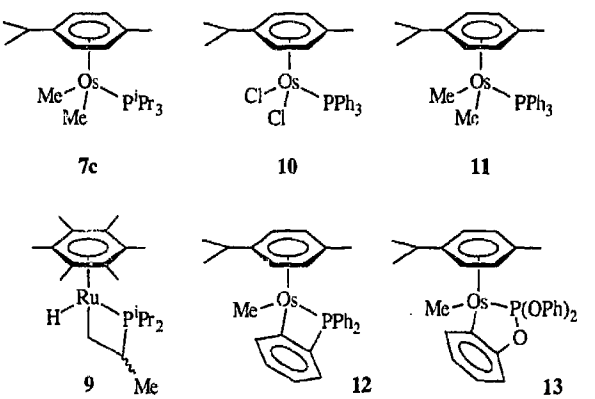

Scheme 5.

differentiated using the following arguments: No NOE was found between the $-CH_2CH(CH_3)P-$ methine proton and the arene protons, but because of an overlap of the $-CH_2CH(CH_3)P-$ methyl protons with one of the phosphine isopropyl methyl signals, their NOE cross peaks with the arene protons cannot be unambiguously assigned. Nevertheless, it can be concluded that structure **8A** is more likely to represent the true form of the metallacycle. This is corroborated by the very similar vicinal H,H-coupling of H^A and H^B with the $-CH_2CH(CH_3)P-$ methine proton (10.8 and 10.0 Hz, respectively) which is only compatible with a quasi-axial position of the latter proton in the postulated puckered four-membered ring. The ^{187}Os NMR chemical shift ($\delta = -3554$ ppm) is in agreement with monoalkylation (cf. δ(**4a**) $= -3605$ ppm; δ(**6d**) $= -3787$ ppm), and the relatively small Os,P coupling constant ($^2J(^{187}Os,^{31}P) = 210$ Hz) appears to reflect a reduced s-character in the bonds of the strained four-membered metallacycle.

Intramolecular attack of a phosphine substituent in osmium alkylation reactions was described for (*p*-cymene)$OsCl_2PPh_3$ when reacted with Al_2Me_6, where one of the phenyl groups became *ortho*-metallated [6] and the monomethyl complex was shown to be the first intermediate. The closest analogue to our complex **8**, however, is the metallacycle **9** obtained from $(C_6Me_6)RuCl(H)P^iPr_3$ [20].

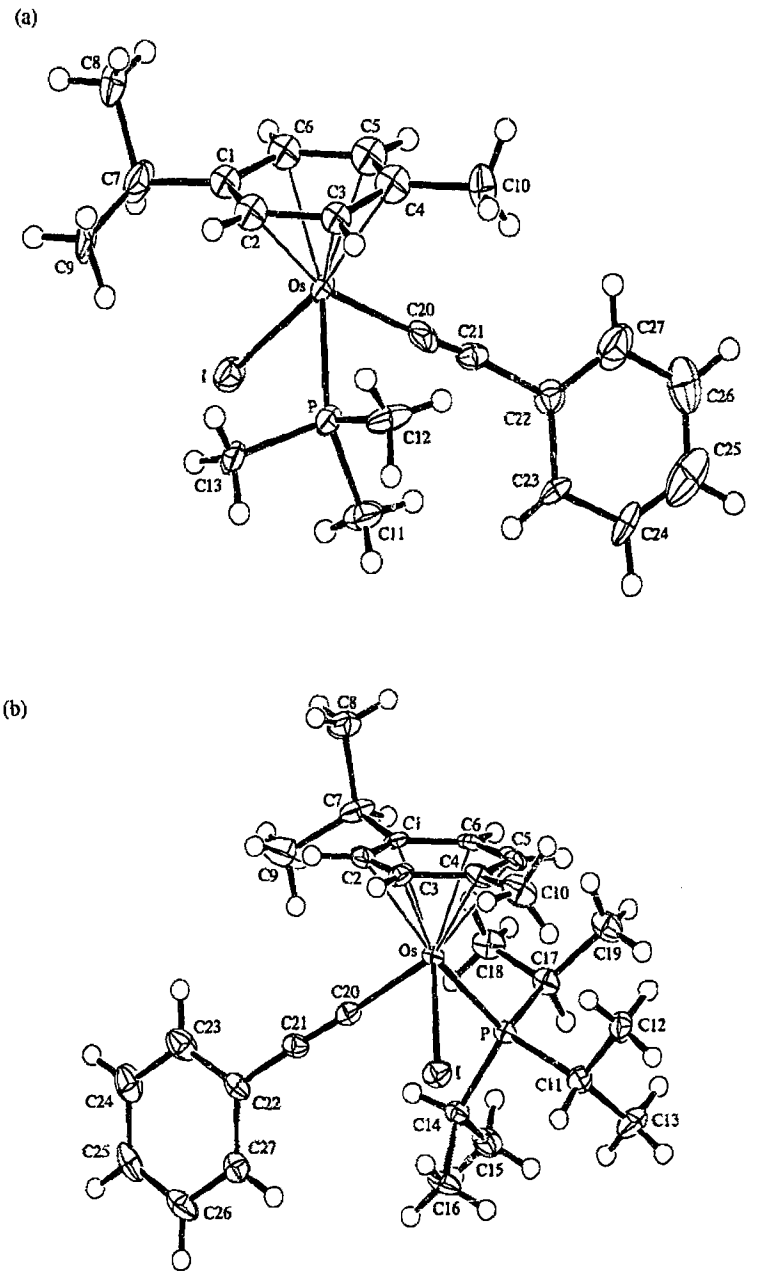

Fig. 1. ORTEP drawings [25] of the molecular structures of (a) **3a** and (b) **3c** (50% probability ellipsoids; arbitrary spheres for H-atoms).

In our case, the formation of the metallacycle **8** was shown by a low-temperature, time-dependent study of the ^{1}H and ^{31}P NMR spectra to proceed via the monomethyl complex **6c**. After dissolving **1c** in toluene-d_8 in an NMR-tube, the solution was deep-frozen, a few drops of Al_2Me_6 in the same solvent were added and the tube was sealed under vacuum. Just before insertion into the NMR probe head, the mixture was brought to thawing temperature to facilitate shimming and tuning. The ^{31}P NMR at 228 K first showed a signal at $\delta = -10.3$ ppm that gradually became weaker in favour of a new signal at $\delta = -34.1$ ppm (273 K) which emanates from the metallacycle **8**. In a second experiment carried out in a flask under the same conditions, the reaction mixture was quenched with aqueous acetone at low temperature shortly after thawing. After column chromatography, a mixture of the mono- and dimethylated complexes **6c** and **7c** (~ 1:1), respectively, was isolated, as shown by ^{1}H, ^{13}C and ^{31}P NMR. There was no trace of the metallacycle **8** in this quenched reaction product (Scheme 3). While **6c** shows an unsymmetric ABCD pattern for the *p*-cymene ring protons, which indicates a chiral osmium atom, the spectrum of the dimethylated product **7c** is of the symmetrical AA'BB' type. This criterion also applies to the isopropyl methyl groups [6].

In the same way, we were able to show that the reaction described by Cabeza and Maitlis [6], in which (*p*-cymene)$OsCl_2PPh_3$ (**10**) reacts with Al_2Me_6 to yield the *ortho*-metallated metallacycle **12**, proceeds via the dimethylated complex **11** (Scheme 5). The corresponding triphenylphosphite complex, however, reacts much faster to yield the analogous *ortho*-metallated product **13**, and mono- or dimethylated intermediates could not be detected. From the above experiments, it can therefore be concluded that osmium mono- or dimethylation precedes formation of the various cyclometallated products that can be considered as intramolecular trans-alkylation products formed under the influence of the Lewis acid reagent Al_2Me_6.

2.3. Molecular structures of (3a) and (3c)

As only four structures have been reported for osmium complexes with σ-bonded acetylene ligands [21–24], and none incorporate an arene ligand, we have determined the crystal structures of (*p*-cymene)$OsI(C{\equiv}CPh)PMe_3$ (**3a**) and (*p*-cymene)$OsI(C{\equiv}CPh)P^iPr_3$ (**3c**) by X-ray diffraction. Selected bond lengths and angles are given in Table 1 and views of the molecules are given in Fig. 1.

Each structure has the usual piano-stool structure exhibited by π-arene metal tri-ligand complexes, with the Os-atom adopting a quasi-octahedral coordination in which the bond angles between the non-arene ligands are in the range 85–90°. The Os–P bond lies approximately perpendicular to the direction of the ring substituents. The principal difference between the two structures is that the *p*-cymene ring in **3a** is rotated approximately 180° about the Os-arene axis relative to its orientation in **3c**. Although the conformation of the molecule of **3a** has been clearly elucidated, the relatively poor quality of the crystals has led to reduced accuracy of the atomic parameters (see Section 4) and any trends in the geometric parameters of **3a** should be treated cautiously, particularly the bond lengths around the alkynyl ligand. The results for **3c** are of a higher quality. The Cambridge Structural Database (CSD, October 1996 version) [26] shows that the mean Os–P bond lengths for osmium complexes with PMe_3 ligands is 2.334(5) Å (50 entries), while for P^iPr_3 ligands, the mean is 2.392(8) Å (47 entries). The Os–P bond lengths in **3a** and **3c** correlate well with these values and reflect the relative steric demands of these phosphine ligands. The Os–I bond lengths are also normal. In **3c**, the Os–C(20) and C(20)≡C(21) bond lengths and the angles, Os–C(20)–C(21) and C(20)–C(21)–C(22), which deviate only slightly from linearity, are all similar to the corresponding parameters in the other osmium complexes with terminal alkynyl ligands [21–24]. The corresponding values in **3a** are probably unreliable. The *p*-cymene ring in **3c** is planar (maximum deviation of the ring carbon atoms from their mean plane is 0.011(6) Å), but the isopropyl and methyl substituents are bent significantly out of the plane and away from the osmium atom (deviations from the ring plane of C(7) and C(10) are 0.197(6) and 0.059(6) Å, respectively). Such deviations, both towards and away from the metal, are

Table 1
Selected interatomic distances (Å) and bond angles (°) for **3a** and **3c**

Compound	3a	3c
Os–I	2.746(2)	2.7577(8)
Os–P	2.334(5)	2.393(2)
Os–C(1)	2.32(2)	2.248(6)
Os–C(2)	2.27(2)	2.238(6)
Os–C(3)	2.15(2)	2.246(6)
Os–C(4)	2.18(2)	2.311(6)
Os–C(5)	2.19(2)	2.288(6)
Os–C(6)	2.29(2)	2.220(6)
Os–C(20)	2.15(3)	2.016(6)
C(20)–C(21)	1.00(3)	1.209(8)
C(1)–C(2)	1.42(3)	1.424(9)
C(1)–C(6)	1.47(3)	1.402(8)
C(2)–C(3)	1.47(3)	1.376(9)
C(3)–C(4)	1.42(3)	1.473(9)
C(4)–C(5)	1.40(3)	1.373(9)
C(5)–C(6)	1.46(3)	1.454(9)
I–Os–P	86.5(2)	89.40(4)
I–Os–C(20)	86.6(6)	85.0(2)
P–Os–C(20)	85.5(6)	87.1(2)
Os–C(20)–C(21)	177(2)	177.9(5)
C(20)–C(21)–C(22)	170(3)	174.1(6)

Table 2
^{187}Os, ^{31}P and ^{17}O chemical shifts of [(*p*-cymene)OsI(CO)PR_3][PF_6] (**2a–f**)

R	Product	$\delta(^{187}Os)$ [ppm]	$\delta(^{31}P)$ [ppm]	$\delta(^{17}O)$ [ppm]
Me_3	**2a**	−4430	−39.3	326.0
Bu_3	**2b**	−4403	−15.8	330.3
$^iPr_3$	**2c**	−4246	16.3	337.6
Cy_3	**2d**	−4215	8.8	338.9
$MePh_2$	**2e**	−4325	−20.1	339.2
Ph_3	**2f**	−4217	−3.8	331.6

frequently observed among 85 *p*-cymene metal complexes found in the CSD. The *p*-cymene ring in **3a** is slightly less planar (max. deviation is 0.05(2) Å), although folding about a particular axis is not discernible, and the isopropyl and methyl substituents lie only 0.06(2) and 0.04(2) Å from the mean ring plane. In each compound, the bond lengths around the arene ring are irregular with the C–C distances varying from 1.376(9) to 1.473(9) Å in **3c**. The *p*-cymene rings are also tilted slightly about the Os-arene axis, the longest Os–C bonds being approximately *trans* to the alkynyl ligand. A similar tilting has been observed in (*p*-cymene)$OsCl_2$(phosphine) complexes [3].

3. Multinuclear NMR studies

The ^{187}Os, ^{31}P and ^{17}O NMR chemical shifts of the cationic carbonyl complexes **2a–f** are listed in Table 2. The range of the ^{187}Os shielding data ($\Delta\delta = 215$ ppm) is much smaller than for the parent diiodo complexes **1a–f** ($\Delta\delta = 572$ ppm) or the corresponding dichloro complexes ($\Delta\delta = 529$ ppm) [3]. The linear dependence of $\delta(^{187}Os)$ on the phosphine cone angle Θ [27] observed for the diiodo compounds is less straightforward in the cationic monocarbonyl complexes (Fig. 2). Whereas the aliphatic phosphine complexes **2a–d** behave analogously to the uncharged dichloro- and diiodo complexes [3], the diphenylmethyl- and triphenylphosphine complexes deviate from this linear correlation. However, when plotted against Tolman's electronic parameter χ [28], the ^{187}Os chemical shifts of **2a**, **2e** and **2f** steadily increase with increasing χ. Thus, the steep increase of $\delta(^{187}Os)$ (decreased shielding) for the aromatic phosphine complexes results from steric and electronic deshielding effects.

As expected, the strong σ-donor/π-acceptor ligand CO also reflects the above effects in the ^{17}O chemical shifts of the terminal oxygen atom. For the aliphatic phosphine complexes, ^{17}O shielding decreases as the phosphine becomes a weaker coordinating ligand, i.e., Me > ^{n}Bu > ^{i}Pr > Cy and all six complexes also exhibit a fairly good correlation ($r = 0.976$) of $\delta(^{17}O)$ with Tolman's steric parameter Θ (Fig. 3). In contrast,

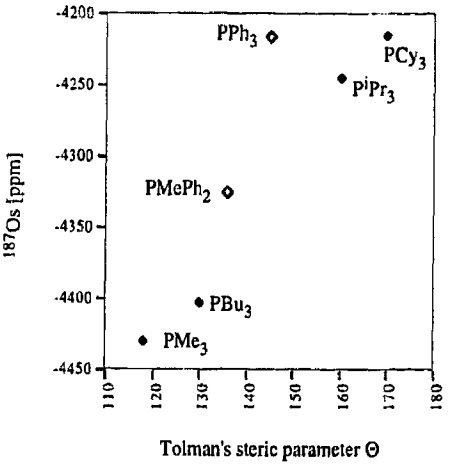

Fig. 2. Correlation of $\delta(^{187}Os)$ with Tolman's steric parameter Θ for complexes **2a–f**.

the ^{13}CO chemical shifts ($\delta = 173$–176 ppm) and $\nu(C{\equiv}O)$ stretching wave numbers (1991–2012 cm^{-1}) do not show any regular trends (see Section 4).

The ^{187}Os NMR shielding in the three alkynyl complexes **3a**, **3c** and **3f** ($\Delta\delta \approx 400$ ppm, Section 4) shows the same sensitivity to the phosphine ligand as the diiodo complexes of type **1** and their corresponding dichloro complexes [3]. There is also a linear dependence on the Tolman angle Θ.

Since alkylation of the parent diiodoosmium complexes **1a–f** has proven difficult, we were unable to synthesise a series of (*p*-cymene)OsI(R)PR'_3 complexes analogous to the $CpFe(CO)_2R$ and $CpFe(CO)(R)PR'_3$ series [4], and therefore, it was not possible to study the Os–C bond in detail by means of ^{187}Os shielding and $^{187}Os,^{13}C$ spin coupling. A comparison of the ^{187}Os NMR data (Section 4) of (*p*-cymene)OsI(Et)PMe_3 (**4a**) ($\delta = -3605$ ppm, $J(^{187}Os,^{31}P) = 288$ Hz) and of (*p*-cymene)OsI(Me)PCy_3 (**6d**) ($\delta = -3787$ ppm, $J(^{187}Os,^{31}P) = 273$ Hz) with those of metallacycle **8**

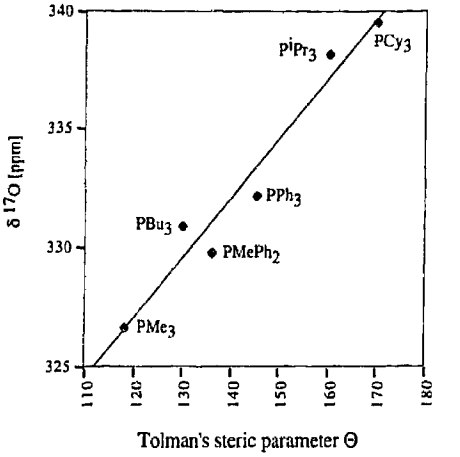

Fig. 3. Correlation of $\delta(^{17}O)$ with Tolman's steric parameter Θ for complexes **2a–f** ($r = 0.976$).

Table 3
$\delta(^{187}Os)$ and coupling constants of compounds $Cp/Cp^* Os(CO)_2Me$ (**14**) and (**15**)

Compound	Ligand	$\delta(^{187}Os)$ [ppm]	$^1J(^{187}Os,^{13}C)$ [Hz]	$^2J(^{187}Os,^1H)$ [Hz]
14	Cp	−5340	48.9	5.7
15	Cp^*	−4985	51.5	5.5

($\delta = -3554$ ppm, $J(^{187}Os,^{31}P) = 210$ Hz) reveals the typical chemical shift range for alkylated osmium complexes [9–11].

However, we have synthesised $CpOs(CO)_2Me$ (**14**) and $Cp^* Os(CO)_2Me$ (**15**) [5,29,30] and determined the ^{187}Os chemical shifts and $^{187}Os,^{13}C$ coupling constants (Table 3). These $\delta(^{187}Os)$ values differ by +355 ppm whereby the osmium atom of the Cp complex is more shielded in contrast to the corresponding iron complexes $Cp/Cp^* Fe(CO)_2Me$ which have a $\Delta\delta(^{57}Fe)$ value of −43 ppm [31,5]. Since the stronger donor ligand Cp^* induces deshielding of the osmium nucleus, the steric hindrance in coordination is the dominant effect, whereas with the iron complexes, the electronic donor effect of Cp^* appears to be stronger.

The $^{187}Os,^{13}C$ one-bond coupling constants of **14** and **15** are very similar (48.9 and 51.5 Hz, respectively). Os,C coupling constants involving sp^3-carbon atoms are rare. The only other case reported in the literature is for (*p*-cymene)$Os(CH(CO_2Me)_2)(NH\text{-}^tBu)$ (56.6 Hz) [16]. These $^{187}Os,^{13}C$ coupling constants are about five times larger than the $^{57}Fe,^{13}C$ values in $CpFe(CO)_2Me$ (9.6 Hz), $CpFe(CO)_2^{neo}Pent$ (9.1 Hz) and $CpFe(CO)[P(OPh)_3]Me$ (10.4 Hz) [31]. For a better comparison of the Os,C and Fe,C coupling, we have also listed the reduced coupling constants $^1\mathbf{K}(Os,C)$ and $^1\mathbf{K}(Fe,C)$ in Table 4.

The fact that the $^1\mathbf{K}$ values of the pairs of osmium and iron complexes differ by a factor of about seven indicates the dominance of the Fermi contact coupling mechanism [32]. An estimate of the electron density term at the nucleus, $(\Psi(0))^2$, leads to values of 27.7 for $Os^{(I)}$ and 5.1 for $Fe^{(I)}$ [33,34] so that this term accounts for about 80% of the difference in the M,C coupling constants of the osmium and iron complexes. The magnitude of Os,C coupling renders it a promising probe to study the $^{187}Os-^{13}C$ σ-bond. Previous studies of Os–CO spin coupling (80–125 Hz) have already demonstrated the usefulness of this parameter in the investigation of the intramolecular dynamics of osmium carbonyl clusters [14,15] and an extension to catalytically active osmium complexes appears to be promising.

Table 4
Reduced coupling constants $^1\mathbf{K}(M,^{13}C)^a$ of complexes $Cp/Cp^* M(CO)_2Me$

	$^1K(^{187}Os,^{13}C)$ [10^{19} N A^{-2} m^{-3}]	$^1K(^{57}Fe,^{13}C)$ [10^{19} N A^{-2} m^{-3}]
Cp	699	98
Cp^*	736	97

$^aK(M,C) = (4\pi^2 J_{(M,C)})/(h\gamma_M\gamma_C)$.

4. Experimental

4.1. NMR spectra

The ^1H, ^{13}C and ^{31}P NMR spectra of complexes **2a–f**, **3a**, **3c**, **3f**, **4a** and **8** were recorded on Bruker ARX-300 and AC-300 NMR spectrometers at 300 MHz, 75 MHz and 121 MHz, respectively. The spectra of **6c**, **6d**, **7c** and the ^{31}P NMR spectrum of **13** were obtained on a Bruker AM-400 at 400 MHz and 162 MHz, respectively.

The inverse detected ^{187}Os NMR spectra were measured on the AM-400 spectrometer at 9 MHz using the HMQC technique as previously described [3]. The ^{17}O NMR spectra were recorded on a Bruker AMX-600 spectrometer at 81 MHz, as well as the ^1H and ^{13}C spectra of **13** at 600 MHz and 151 MHz, respectively. The $^{187}Os,^1H$ and $^{187}Os,^{13}C$ coupling constants for complexes **14** and **15** were determined in a ^{13}C-filtered ($^1H,^{187}Os$)-HMQC correlation spectrum [35] on the AMX-600. All NMR spectra were recorded at 300 K. ^1H and ^{13}C NMR spectra were referenced relative to TMS, the ^{31}P spectra relative to H_3PO_4 (85%), the ^{17}O spectra relative to D_2O, and the ^{187}Os spectra relative to OsO_4. Chemical shifts are listed in ppm, coupling constants in Hz. The first mentioned multiplicities in the ^{13}C NMR data are from DEPT experiments.

4.2. X-ray structure determination for (3a) and (3c)

All measurements were made on a Rigaku AFC5R diffractometer using graphite-monochromated Mo Kα radiation ($\lambda = 0.71069$ Å) and a 12 kW rotating anode generator. The intensities of three standard reflections were measured after every 150 reflections and remained stable throughout each data collection. The intensities were corrected for *Lorentz* and polarisation effects. Absorption corrections based on ψ-scans of several reflections were applied [36]. Analytical absorption corrections produced inferior results. The structures were solved by Patterson methods using Dirdif-92 [37] for **3a** and Shelxs-86 [38] for **3c**, which in each case revealed the positions of the Os and I-atoms. All remaining non-hydrogen atoms were located in Fourier expansions of the Patterson solutions. The Texsan crystallographic software package [39] was used to refine each structure on F using full-matrix least-squares procedures, which minimised the function $\Sigma w(|F_o| - |F_c|)^2$, where $w =$

$[\sigma^2(F_o) + (0.005F_o)^2]^{-1}$. The weighting scheme was based on counting statistics and included a factor to downweight the intense reflections. Plots of $\Sigma w(|F_o| - |F_c|)^2$ vs. $|F_o|$, reflection order in the data collection, $\sin\theta/\lambda$ and various classes of indices showed no unusual trends. The data collection and refinement parameters are given in Table 5.

The crystal of **3a** was a very thin plate of poor quality and produced broad reflection profiles. The form of the crystal made it difficult to carry out accurate absorption corrections and the quality of the data has reduced the accuracy of the atomic positional parameters, bond lengths and angles. It was necessary to refine the C-atoms of the arene ring with only isotropic displacement parameters. All other non-hydrogen atoms were refined anisotropically and the H-atoms were fixed in geometrically calculated positions [d(C–H) = 0.95 Å] with fixed isotropic temperature factors assigned to be 1.2 U_{eq} of the parent C-atom. A correction for secondary extinction was not applied, but the reflection 400 was omitted because of suspected extinction effects. Peaks of residual electron density of up to 4.1 and 2.2 e Å^{-3} remained in the final difference electron density map close to the Os and I-atoms, respectively. These can be attributed to the data quality and the difficulty of applying accurate absorption corrections. The direction of the polar axis was determined by refinement of the completed structure together with the absolute structure parameter [40,41] using the program Crystals [42]. This parameter converged to 0.01(5), which confidently confirms that the refined atomic coordinates, as listed in Table 6, correspond with the true direction of the polar axis.

For **3c**, the non-hydrogen atoms were refined anisotropically. All of the H-atoms were fixed in geometrically calculated positions [d(C–H) = 0.95 Å] and they were assigned fixed isotropic temperature factors with a value equal to 1.2 U_{eq} of the atom to which each was bonded. A correction for secondary extinction was applied and the largest peaks of residual electron density were near the Os and I-atoms. The atomic coordinates are given in Table 7.

Neutral atom scattering factors for non-hydrogen atoms were taken from Maslen et al. [43], and the scattering factors for H-atoms were taken from Stewart et al. [44]. Anomalous dispersion effects were included

Table 5
Crystallographic data for **3a** and **3c**

Compound	**3a**	**3c**
Crystallised from	CH_2Cl_2 / *n*-pentane	CH_2Cl_2 / *n*-pentane
Empirical formula	$C_{21}H_{28}IOsP$	$C_{27}H_{40}IOsP$
Formula weight	628.53	712.69
Crystal colour, habit	orange, plate	red, prism
Crystal dimensions (mm)	0.05×0.23×0.30	0.20×0.28×0.32
Temperature (K)	173(1)	173(1)
Crystal system	orthorhombic	monoclinic
Space group	$Pna2_1$	$P2_1/c$
Z	4	4
Reflections for cell determination	25	25
2θ range for cell determination (°)	37–40	39–40
a (Å)	27.812(14)	14.593(3)
b (Å)	7.451(5)	8.780(2)
c (Å)	10.174(4)	21.582(3)
β (°)	90	107.72(1)
V (Å^3)	2108(2)	2634.0(9)
F(000)	1192	1384
D_x (g cm^{-3})	1.980	1.797
μ(Mo Kα) (mm^{-1})	7.586	6.083
Scan type	ω	$\omega/2\theta$
$2\theta_{(max)}$ (°)	55	60
Transmission factors (min; max)	0.377; 1.000	0.854; 1.000
Total reflections measured	3335	8431
Symmetry independent reflections	2564	7678
R_{merge}	0.075	0.074
Reflections used ($I > 2\sigma(I)$)	2019	5873
Parameters refined	186	272
R	0.0502	0.0376
R_w	0.0557	0.0361
Goodness of fit	1.934	1.809
Secondary extinction coefficient	–	5(7)×10^{-8}
Final Δ_{max}/σ	0.0002	0.0004
$\Delta\rho$ (max; min) (e Å^{-3})	4.05; −2.99	1.86; −2.43

Table 6
Fractional atomic coordinates and equivalent isotropic temperature factors for **3a**

Atom	x	y	z	U_{eq} (Å^2)[a]
Os	0.12496(3)	0.10953(9)	0.46834[†]	0.0207(2)
I	0.18064(5)	0.3949(2)	0.3909(2)	0.0302(4)
P	0.1900(2)	0.0232(8)	0.5988(5)	0.025(2)
C(1)	0.1133(8)	0.025(3)	0.251(2)	0.027(5)[b]
C(2)	0.1274(9)	−0.126(3)	0.327(2)	0.032(5)[b]
C(3)	0.1031(7)	−0.166(2)	0.452(2)	0.025(5)[b]
C(4)	0.0622(8)	−0.064(3)	0.489(3)	0.036(5)[b]
C(5)	0.0488(9)	0.089(3)	0.417(2)	0.036(6)[b]
C(6)	0.0730(8)	0.138(3)	0.295(2)	0.030(5)[b]
C(7)	0.140(1)	0.084(3)	0.126(2)	0.040(8)
C(8)	0.106(1)	0.038(4)	0.010(2)	0.046(9)
C(9)	0.189(1)	0.003(4)	0.111(2)	0.06(1)
C(10)	0.036(1)	−0.114(4)	0.620(2)	0.05(1)
C(11)	0.2131(9)	0.186(3)	0.715(2)	0.035(7)
C(12)	0.1798(9)	−0.175(3)	0.698(2)	0.040(8)
C(13)	0.2437(8)	−0.045(4)	0.508(2)	0.040(8)
C(20)	0.1040(8)	0.272(3)	0.633(2)	0.033(7)
C(21)	0.0925(8)	0.344(3)	0.711(2)	0.023(6)
C(22)	0.0801(9)	0.434(3)	0.845(2)	0.029(7)
C(23)	0.1186(9)	0.494(4)	0.929(2)	0.035(8)
C(24)	0.106(1)	0.558(4)	1.048(2)	0.05(1)
C(25)	0.062(1)	0.576(4)	1.089(3)	0.06(1)
C(26)	0.023(1)	0.521(4)	1.010(3)	0.05(1)
C(27)	0.033(1)	0.450(4)	0.889(3)	0.05(1)

[a] U_{eq} is defined as one third of the trace of the orthogonalised U^{ij} tensor.
[b] Atom refined isotropically only.

Table 7
Fractional atomic coordinates and equivalent isotropic temperature factors for **3c**

Atom	x	y	z	U_{eq} (Å^2)[a]
Os	0.37309(2)	0.90450(3)	0.08168(1)	0.01516(7)
I	0.43914(3)	1.18986(5)	0.12755(2)	0.0250(1)
P	0.2444(1)	0.9326(2)	0.12794(8)	0.0165(5)
C(1)	0.3789(5)	0.6902(7)	0.0260(3)	0.021(2)
C(2)	0.4503(5)	0.7931(7)	0.0187(3)	0.025(2)
C(3)	0.5188(5)	0.8537(7)	0.0717(3)	0.023(2)
C(4)	0.5233(4)	0.8117(7)	0.1386(3)	0.023(2)
C(5)	0.4553(5)	0.7116(7)	0.1463(3)	0.025(2)
C(6)	0.3820(5)	0.6525(7)	0.0897(3)	0.022(2)
C(7)	0.3101(5)	0.6058(8)	−0.0306(3)	0.030(2)
C(8)	0.3644(5)	0.4724(8)	−0.0482(4)	0.033(3)
C(9)	0.2642(8)	0.703(1)	−0.0905(4)	0.077(4)
C(10)	0.6023(5)	0.8733(8)	0.1948(4)	0.034(3)
C(11)	0.2826(5)	1.0126(7)	0.2114(3)	0.023(2)
C(12)	0.3753(5)	0.9410(8)	0.2563(3)	0.026(2)
C(13)	0.2041(5)	1.0179(9)	0.2454(3)	0.033(3)
C(14)	0.1441(4)	1.0597(7)	0.0819(3)	0.020(2)
C(15)	0.0434(5)	1.0349(8)	0.0886(3)	0.030(2)
C(16)	0.1700(5)	1.2295(8)	0.0917(4)	0.031(3)
C(17)	0.1749(4)	0.7571(7)	0.1342(3)	0.022(2)
C(18)	0.1327(5)	0.6845(8)	0.0671(4)	0.029(2)
C(19)	0.2261(5)	0.6402(8)	0.1856(4)	0.030(2)
C(20)	0.2895(4)	1.0167(7)	0.0033(3)	0.018(2)
C(21)	0.2407(4)	1.0812(7)	−0.0450(3)	0.020(2)
C(22)	0.1734(4)	1.1524(7)	−0.1013(3)	0.021(2)
C(23)	0.1500(5)	1.0838(8)	−0.1631(4)	0.032(3)
C(24)	0.0802(5)	1.1486(9)	−0.2161(3)	0.034(3)
C(25)	0.0354(5)	1.2790(9)	−0.2087(3)	0.032(2)
C(26)	0.0572(5)	1.3519(8)	−0.1493(4)	0.033(3)
C(27)	0.1253(5)	1.2886(8)	0.0959(3)	0.027(2)

[a] U_{eq} is defined as one third of the trace of the orthogonalised U^{ij} tensor.

in F_{calc} [45]; the values for f' and f'' were those of Creagh and McAuley [46]. Complete tables of atomic coordinates, bond lengths and angles have been deposited with the Cambridge Crystallographic Data Centre. Lists of observed and calculated structure factors and of thermal displacement parameters are available from the authors.

4.3. Preparation

All reactions were performed in dry glassware under an inert gas atmosphere. Solvents were chemically dried and distilled prior to use. The educt complexes **1a–f** were prepared by literature procedures [3].

4.4. Synthesis of [(p-cymene)OsI(CO)PR$_3$][PF$_6$] (2a–f) [7,17]

4.4.1. [(p-Cymene)OsI(CO)PMe$_3$][PF$_6$] (2a)

Reactions and work-up for complexes **2a–f** were performed under a CO-atmosphere.

Under gentle stirring, CO gas was bubbled through a suspension of 325 mg (0.5 mmol) **1a** in 5 ml acetone for 30 min. Then, 126 mg (0.5 mmol) $AgPF_6$ dissolved in 5 ml acetone were added dropwise (ca. 10 min), leading to precipitation of AgI. After stirring for another 5 min, AgI was filtered off and 150 ml Et_2O/hexane (2:1) were added dropwise under constant stirring (ca. 1 h). The precipitated microcrystalline product was filtered off and dried in vacuum to yield 249 mg (0.36 mmol, 72%) of an orange powder.

IR (KBr) ν(C=O) [cm^{-1}] 1998s. **^{1}H NMR** (acetone-d_6): δ 6.91 (dd, ^3J = 7.1, ^4J = 1.3, 1H, Ar), 6.86 (dd, ^3J = 6.4, ^4J = 1.3, 1H, Ar), 6.66 (d, ^3J = 6.0, 1H, Ar), 6.63 (d, ^3J = 6.6, 1H, Ar), 3.06 (sept, ^3J = 6.9, 1H, Ar–C*H*(CH$_3$)$_2$), 2.71 (s, 3H, Ar–C*H*$_3$), 2.18 (d, $^2J(^{31}P,^1H)$ = 11.3, 9H, P(CH$_3$)$_3$), 1.38 (d, ^3J = 6.8, 3H, Ar–CH(C*H*$_3$)$_2$), 1.38 (d, ^3J = 6.8, 3H, Ar–CH(C*H*$_3$)$_2$). **^{13}C NMR** (acetone-d_6): δ 174.6 (sd, $^2J(^{31}P,^{13}C)$ = 14.9, C=O), 117.3 (s, C(1)), 112.1 (s, C(4)), 98.7 (d, Ar), 96.9 (d, Ar), 95.3 (d, Ar), 88.9 (d, Ar), 33.9 (d, Ar–*C*H(CH$_3$)$_2$), 23.4, 22.7 (q, Ar–CH(*C*H$_3$)$_2$), 20.6 (qd, $^1J(^{31}P,^{13}C)$ = 43.5, P(CH$_3$)$_3$), 19.9 (q, Ar–*C*H$_3$). **^{31}P NMR** (acetone-d_6): δ −39.3. **^{17}O NMR** (CD$_3$CN): δ 326.6. **^{187}Os NMR** (CD$_3$CN): δ −4430 (d, $^1J(^{187}Os,^{31}P)$ = 222).

4.4.2. [(p-Cymene)OsI(CO)P^{n}Bu$_3$][PF$_6$] (2b)

Orange powder. Yield 69%. **IR** (KBr). ν(C=O) [cm^{-1}] 1991s (C=O). **^{1}H NMR** (CD$_3$CN): δ 6.51 (dd, ^3J = 6.7, ^4J = 1.1, 1H, Ar), 6.32 (d, ^3J = 6.2, 1H, Ar), 6.27 (dd, ^3J = 6.9, ^4J = 1.1, 1H, Ar), 6.24 (dd, ^3J = 6.2, ^4J = 2.0, 1H, Ar), 2.85 (sept, ^3J = 6.9, 1H, Ar–C*H*(CH$_3$)$_2$), 2.59 (s, 3H, Ar–C*H*$_3$), 2.27–2.08 (m, 6H, P(CH$_2$–)$_3$), 1.50–1.31 (m, 12H, P(CH$_2$C*H*$_2$C*H*$_2$–)$_3$), 1.31 (d, ^3J = 7.1, 6H, Ar–CH(C*H*$_3$)$_2$), 0.93 (t, ^3J = 6.9, 9H, P[(CH$_2$)$_3$C*H*$_3$]$_3$). **^{13}C NMR** (CD$_3$CN): δ 174.0 (sd, $^2J(^{31}P,^{13}C)$ = 14.7, C=O), 117.9 (s, C(1)), 114.9 (s, C(4)), 97.6 (d, Ar), 96.2 (d, Ar), 94.7 (d, Ar), 88.7 (d, Ar), 33.2 (d, Ar–*C*H(CH$_3$)$_2$), 29.7 (td, $^1J(^{31}P,^{13}C)$ = 37.6, P(CH$_2$–)$_3$), 26.9 (td, $^2J(^{31}P,^{13}C)$ = 3.9, P(CH$_2$*C*H$_2$–)$_3$), 24.5 (td, $^3J(^{31}P,^{13}C)$ = 14.8, P(CH$_2$CH$_2$*C*H$_2$)$_3$), 24.7, 21.1 (q, Ar–CH(*C*H$_3$)$_2$), 20.2 (q, Ar–*C*H$_3$), 14.0 (q, P[(CH$_2$)$_3$*C*H$_3$]$_3$). **^{31}P NMR** (CD$_3$CN): δ −15.8. **^{17}O NMR** (CD$_3$CN): δ 330.9. **^{187}Os NMR** (CD$_3$CN): δ −4403 (d, $^1J(^{187}Os,^{31}P)$ = 223).

4.4.3. [(p-Cymene)OsI(CO)P^{i}Pr$_3$][PF$_6$] (2c)

Orange powder. Yield 74%. Found (calc.): C: 30.28 (30.62), H: 4.71 (4.50). **IR** (KBr) ν(C=O) [cm^{-1}] 1998s. **^{1}H NMR** (CD$_3$CN): δ 6.61 (d, ^3J = 6.7, 1H, Ar), 6.49 (d, ^3J = 6.4, 1H, Ar), 6.46 (d, ^3J = 6.3, 1H, Ar), 6.31 (d, ^3J = 6.8, ^4J = 1.0, 1H, Ar), 2.87 (sept, ^3J = 6.9, 1H, Ar–C*H*(CH$_3$)$_2$), 2.78 (dsept, $^2J(^{31}P,^1H)$ = 9.9, ^3J = 7.2, 3H, P(C*H*(CH$_3$)$_2$)$_3$), 2.63 (s, 3H, Ar–C*H*$_3$), 1.34–1.25 (m, 24H, Ar–CH(C*H*$_3$)$_2$, P(CH(C*H*$_3$)$_2$)$_3$). **^{13}C NMR** (CD$_3$CN): δ 175.2 (sd, $^2J(^{31}P,^{13}C)$ = 13.5, C=O), 118.7 (s, C(1)), 117.7 (s,

C(4)), 97.5 (d, Ar), 95.4 (d, Ar), 93.6 (d, Ar), 88.7 (d, Ar), 33.2 (d, Ar–*C*H(CH_3)$_2$), 30.8 (dd, $^1J(^{31}P,^{13}C)$ = 30.7, P(*C*H(CH_3)$_2$)$_3$), 25.4 (q, Ar–CH(*C*H_3)$_2$), 20.7, 20.2 (q, Ar–*C*H_3) 20.5, 20.4 (q, PCH(*C*H_3)$_2$). **^{31}P NMR** (CD_3CN): δ 16.3. **^{17}O NMR** (CD_3CN): δ 338.2. **^{187}Os NMR** (CD_3CN): δ −4246 (d, $^1J(^{187}Os,^{31}P)$ = 229).

4.4.4. [(p-Cymene)OsI(CO)PCy$_3$][PF$_6$] (2d)

Orange powder. Yield 56%. **IR** (KBr) ν(C=O) [cm^{-1}] 1989s. **^{1}H NMR** (CD_3CN): δ 6.58 (d, ^3J = 6.7, 1H, Ar), 6.47 (sb, 2H, Ar), 6.34 (d, ^3J = 6.6, 1H, Ar), 2.85 (sept, ^3J = 6.9, 1H, Ar–C*H*(CH_3)$_2$), 2.61 (s, 3H, Ar–CH_3), 2.50–2.39 (m, 3H, P(Cy)$_3$, (C(1)*H*)$_3$), 2.08–2.03 (m, 3H, P(Cy)$_3$), 1.94–1.83 (m, 6H, P(Cy)$_3$), 1.77–1.69 (m, 6H, P(Cy)$_3$), 1.48–1.21 (m, 15H, P(Cy)$_3$), 1.35 (d, ^3J = 6.8, 3H, Ar–CH(CH_3)$_2$), 1.33 (d, ^3J = 6.3, 3H, Ar–CH(CH_3)$_2$). **^{13}C NMR** (CD_3CN): δ 175.5 (sd, $^2J(^{31}P,^{13}C)$ = 13.3, CO), 120.3 (s, Ar, C(1)), 117.0 (s, Ar, C(4)), 97.4 (d, Ar), 94.5 (d, Ar), 92.1 (d, Ar), 88.4 (d, Ar), 40.4 (dd, $^1J(^{31}P,^{13}C)$ = 27.5, P(Cy)$_3$, C(1)), 33.3 (d, Ar–*C*H(CH_3)$_2$), 31.0 (td, $^3J(^{31}P,^{13}C)$ = 31.8, P(Cy)$_3$, C(3), C(5)), 28.1 (td, $^2J(^{31}P,^{13}C)$ = 11.9, P(Cy)$_3$, C(2), C(6)), 26.9 (t, P(Cy)$_3$, C(4)), 25.7, 20.4 (q, Ar–CH(*C*H_3)$_2$), 20.2 (q, Ar–*C*H_3). **^{31}P NMR** (CD_3CN): δ 8.8. **^{17}O NMR** (CD_3CN): δ 339.5. **^{187}Os NMR** (CD_3CN): δ −4215 (d, $^1J(^{187}Os,^{31}P)$ = 226).

4.4.5. [(p-Cymene)OsI(CO)PMePh$_2$][PF$_6$] (2e)

Yellow-brownish powder. Yield 61%. **IR** (KBr) ν(C=O) [cm^{-1}] 2012s. **^{1}H NMR** (CD_3CN): δ 7.63–7.51 (m, 10H, PMe*Ph*$_2$), 6.45 (d, ^3J = 6.5, 1H, Ar), 6.25 (d, ^3J = 6.4, 1H, Ar), 6.14 (d, ^3J = 6.0, 1H, Ar), 5.93 (d, ^3J = 6.1, 1H, Ar), 2.70 (sept, ^3J = 6.9, 1H, Ar–C*H*(CH_3)$_2$), 2.63 (d, $^2J(^{31}P,^1H)$ = 10.5, 3H, P*Me*Ph$_2$,), 2.47 (s, 3H, Ar–CH_3), 1.15 (d, ^3J = 6.9, 3H, Ar–CH(CH_3)$_2$), 1.12 (d, ^3J = 7.0, 3H, Ar–CH(CH_3)$_2$). **^{13}C NMR** (CD_3CN): δ 173.4 (sd, $^2J(^{31}P,^{13}C)$ = 15.5, C=O), 134.5 (sd, $^1J(^{31}P,^{13}C)$ = 52.6, PMe*Ph*$_2$, C(1)), 133.9 (dd, $^3J(^{31}P,^{13}C)$ = 9.8, PMe*Ph*$_2$, C(3), C(5)), 133.1 (d, PMe*Ph*$_2$, C(4)), 130.1 (dd, $^2J(^{31}P,^{13}C)$ = 11.6, PMe*Ph*$_2$, C(2), C(6)), 129.9 (dd, $^2J(^{31}P,^{13}C)$ = 11.8, PMe*Ph*$_2$, C(2), C(4)), 119.0 (s, Ar, C(1)), 115.7 (s, Ar, C(4)), 97.4 (d, Ar), 96.4 (d, Ar), 96.1 (d, Ar), 91.2 (d, Ar), 32.7 (d, Ar–*C*H(CH_3)$_2$), 24.5, 23.4 (q, Ar–CH(*C*H_3)$_2$), 20.8 (qd, $^1J(^{31}P,^{13}C)$ = 44.9, P*Me*Ph$_2$), 19.7 (q, Ar–*C*H_3). **^{31}P NMR** (CD_3CN): δ −20.1. **^{17}O NMR** (CD_3CN): δ 329.8. **^{187}Os NMR** (CD_3CN): δ −4325 (d, $^1J(^{187}Os,^{31}P)$ = 234).

4.4.6. [(p-Cymene)OsI(CO)PPh$_3$][PF$_6$] (2f)

Yellow-orange powder. Yield 59%. Found (calc.): C: 39.03 (39.29), H: 3.53 (3.30). **IR** (KBr) ν(C=O) [cm^{-1}] 2007s. **^{1}H NMR** (CD_3CN): δ 7.68–7.45 (m, 15H, PPh$_3$), 6.58 (dd, ^3J = 6.7, ^4J = 1.3, 1H, Ar), 6.35 (dd, ^3J = 6.7, ^4J = 1.5, 1H, Ar), 6.10 (dd, ^3J = 6.3, ^4J = 1.4, 1H, Ar), 5.56 (dd, ^3J = 6.2, 1H, Ar), 2.95 (sept, ^3J = 6.9, 1H, Ar–C*H*(CH_3)$_2$), 2.22 (s, 3H, Ar–CH_3), 1.30 (d, ^3J = 6.9, 3H, Ar–CH(CH_3)$_2$), 1.27 (d, ^3J = 6.9, 3H, Ar–CH(CH_3)$_2$). **^{13}C NMR** (CD_3CN): δ 173.4 (sd, $^2J(^{31}P,^{13}C)$ = 15.6, C=O), 135.2 (dd, $^3J(^{31}P,^{13}C)$ = 10.3, PPh$_3$, C(3), C(5)), 133.4 (dd, $^4J(^{31}P,^{13}C)$ = 2.3, PPh$_3$, C(4)), 132.0 (sd, $^1J(^{31}P,^{13}C)$ = 61.7, PPh$_3$, C(1)), 130.0 (dd, $^2J(^{31}P,^{13}C)$ = 11.3, PPh$_3$, C(2), C(6)), 119.6 (s, Ar, C(1)), 119.4 (s, Ar, C(4)), 98.6 (d, Ar), 97.2 (d, Ar), 97.0 (d, Ar), 90.4 (d, Ar), 32.9 (d, Ar–*C*H(CH_3)$_2$), 24.2, 21.9 (q, Ar–CH(*C*H_3)$_2$), 19.4 (q, Ar–*C*H_3). **^{31}P NMR** (CD_3CN): δ −3.8. **^{17}O NMR** (CD_3CN): δ 332.2. **^{187}Os NMR** (CD_3CN): δ −4217 (d, $^1J(^{187}Os,^{31}P)$ = 242).

4.5. Synthesis of (p-cymene)OsI(phenylacetylene)PR$_3$ (3a, c, f)

4.5.1. (p-Cymene)OsI(phenylethynyl)PMe$_3$ (3a)

Under an argon atmosphere, 40 ml of phenylacetylene were dissolved in 5 ml acetone and cooled to −78°C (dry-ice/acetone). The cooled solution was added dropwise via a syringe into a Schlenk-tube, containing 196 mg (0.3 mmol) **1b** and 76 mg (0.3 mmol) $AgPF_6$. The orange-red reaction mixture was stirred for about 5 min at −78°C. After warming up to room temperature, the precipitated AgI was filtered off and the filtrate was vacuum-evaporated to leave a brown oil. The raw product was purified by column chromatography (alox; Et_2O/acetone (10:1)). The yellow fraction was vacuum-concentrated to ca. 2 ml, *n*-pentane was added to the remaining solution and the mixture was cooled to −20°C to give 68 mg of orange crystals (0.11 mmol, 36%).

^{1}H NMR (CD_3CN): δ 7.32–7.15 (m, 4H, –C≡CPh, H(2), H(3), H(5), H(6)), 7.09–7.04 (m, 1H, –C≡CPh, H(4)), 5.53 (d, ^3J = 5.7, 1H, Ar), 5.47 (d, ^3J = 5.5, 1H, Ar), 5.26 (m, 2H, Ar), 2.98 (sept, ^3J = 6.9, 1H, Ar–C*H*(CH_3)$_2$), 2.43 (s, 3H, Ar–CH_3), 1.86 (d, $^2J(^{31}P,^1H)$ = 10.3, 9H, P(CH_3)$_3$), 1.33 (d, ^3J = 6.9, 6H, Ar–CH(CH_3)$_2$). **^{13}C NMR** (CD_3CN): δ 131.8 (d, –C≡C*Ph*, C(3), C(5)), 128.9 (s, –C≡C*Ph*, C(1)), 127.6 (d, –C≡C*Ph*, C(4)), 124.4 (d, –C≡C*Ph*, C(2), C(6)), 103.7 (s, Os–C≡*C*Ph), 103.4 (s, Ar, C(1)), 91.5 (s, Ar, C(4)), 89.0 (sd, $^2J(^{31}P,^{13}C)$ = 27.2, Os–*C*≡CPh), 83.5 (d, Ar), 82.3 (d, Ar), 79.8 (d, Ar), 77.3 (d, Ar), 31.1 (d, Ar–*C*H(CH_3)$_2$), 22.8, 22.5 (q, Ar–CH(*C*H_3)$_2$), 19.2 (qd, $^1J(^{31}P,^{13}C)$ = 39.9, P(CH_3)$_3$), 18.9 (q, Ar–*C*H_3). **^{31}P NMR** (CD_3CN): δ −48.4. **^{187}Os NMR** (CD_3CN): δ −3931 (d, $^1J(^{187}Os,^{31}P)$ = 248).

4.5.2. (p-Cymene)OsI(phenylethynyl)P^{i}Pr$_3$ (3c)

^{1}H NMR (CD_3CN): δ 7.15–7.00 (m, 4H, –C≡CPh, H(2), H(3), H(5), H(6)), 6.98–6.77 (m, 1H, –C≡CPh, H(4)), 5.62 (d, ^3J = 5.9, 1H, Ar), 5.55 (d, ^3J = 5.8, 1H,

Ar), 5.51 (d, $^3J = 6.0$, 1H, Ar), 5.43 (d, $^3J = 5.6$, 1H, Ar), 2.97 (sept, $^3J = 6.9$, 1H, Ar–C*H*$(CH_3)_2$), 2.85 (dsept, $^2J(^{31}P,^1H) = 9.7$, $^3J = 7.2$, 3H, P(C*H*$(CH_3)_2)_3$), 2.38 (s, 3H, Ar–CH_3), 1.27 (m, 24H, Ar–CH(C$H_3)_2$, P(CH(C$H_3)_2)_3$). **^{13}C NMR** (CD_3CN): δ 131.7 (d, –C≡C*Ph*, C(3), C(5)), 129.1 (s, –C≡C*Ph*, C(1)), 127.5 (d, –C≡C*Ph*, C(2), C(6)), 124.1 (d, –C≡C*Ph*, C(4)), 108.3 (s, Os–C≡*C*Ph), 104.2 (s, Ar, C(1)), 92.8 (s, Ar, C(4)), 85.2 (sd, $^2J(^{31}P,^{13}C) = 23.3$, Os–*C*≡CPh), 84.9 (d, Ar), 83.1 (d, Ar), 80.7 (d, Ar), 75.3 (d, Ar), 30.9 (d, Ar–*C*H$(CH_3)_2$), 28.3 (dd, $^1J(^{31}P,^{13}C) = 26.9$, P(*C*H$(CH_3)_2)_3$), 24.2, 21.9 (q, Ar–CH(*C*$H_3)_2$), 20.6, 20.4 (q, P(CH(*C*$H_3)_2$)), 18.6 (q, Ar–*C*H_3). **^{31}P NMR** (CD_3CN): δ −6.77. **^{187}Os NMR** (CD_3CN): δ −3541 (d, $^1J(^{187}Os,^{31}P) = 256$).

4.5.3. (p-Cymene)OsI(phenylethynyl)PPh$_3$ (3f)

^{1}H NMR (CD_2Cl_2): δ 7.79–7.68 (m, 6H, PPh_3, H(3), H(5)), 7.32–7.23 (m, 9H, PPh_3, H(2), H(4), H(6)), 7.32–7.15 (m, 4H, –C≡CPh, H(2), H(3), H(5), H(6)), 7.09–7.04 (m, 1H, –C≡CPh, H(4)), 5.31 (d, $^3J = 5.6$, 1H, Ar), 5.28 (d, $^3J = 6.4$, 1H, Ar), 5.08 (d, $^3J = 5.7$, 1H, Ar), 4.85 (d, $^3J = 5.7$, 1H, Ar), 2.88 (sept, $^3J = 6.9$, 1H, Ar–C*H*$(CH_3)_2$), 2.10 (s, 3H, Ar–CH_3), 1.20 (d, $^3J = 6.9$, 3H, Ar–CH(C$H_3)_2$), 1.19 (d, $^3J = 6.9$, 3H, Ar–CH(C$H_3)_2$). **^{13}C NMR** (CD_2Cl_2): δ 135.7 (sd, $^1J(^{31}P,^{13}C) = 53.5$, PPh_3, C(1)), 134.5 (dd, $^3J(^{31}P,^{13}C) = 9.5$, PPh_3, C(3), C(5)), 131.6 (d, –C≡C*Ph*, C(3), C(5)), 129.8 (d, PPh_3, C(4)), 128.8 (s, –C≡C*Ph*, C(1)), 127.5 (dd, $^2J(^{31}P,^{13}C) = 10.0$, PPh_3, C(2), C(6)), 127.3 (d, Os–C≡C*Ph*, C(2), C(6)), 124.3 (d, –C≡C*Ph*, C(4)), 108.1 (s, Os–C≡*C*Ph), 106.9 (s, Ar, C(1)), 85.9 (s, Ar, C(4)), 85.5 (sd, $^2J(^{31}P,^{13}C) = 27.2$, Os–*C*≡CPh), 85.5 (d, Ar), 84.7 (d, Ar), 82.6 (d, Ar), 79.0 (d, Ar), 30.6 (d, Ar–*C*H$(CH_3)_2$), 23.4, 21.7 (q, Ar–CH(*C*$H_3)_2$), 17.8 (q, Ar–*C*H_3). **^{31}P NMR** (CD_3CN): δ −13.0. **^{187}Os NMR** (CD_3CN): δ −3694 (d, $^1J(^{187}Os,^{31}P) = 266$).

4.6. Alkylation reactions

4.6.1. Synthesis of (p-cymene)OsI(Et)PMe$_3$ (4a)

Under an argon atmosphere, a suspension of 144 mg (0.22 mmol) **1a** in 2 ml of toluene was cooled to 0°C. With a syringe, 250 ml (0.32 mmol) $AlEt_3$ (1.3 M in hexane) were added dropwise to the red suspension. An immediate colour change to light-orange was observed. The reaction mixture was stirred for 10 min without cooling while **1a** totally dissolved. Then, a mixture of 1.2 ml acetone and 0.05 ml H_2O was added dropwise leading to gas formation and precipitation of a white solid, while the solution turned red. After stirring for another 20 min, the reaction mixture was extracted with Et_2O. From the ether phase, a yellow band could be eluted by column chromatography (alox/Et_2O). This fraction was vacuum-concentrated to ca. 1 ml, 8 ml *n*-pentane were added, and the mixture was cooled to −10°C to yield 35.5 mg (0.06 mmol, 29%) of an orange powder.

^{1}H NMR (CD_2Cl_2): δ 5.01 (d, $^3J = 5.2$, 1H, Ar), 4.98 (d, $^3J = 6.1$, 1H, Ar), 4.85 (d, $^3J = 5.7$, 1H, Ar), 4.54 (d, $^3J = 4.9$, 1H, Ar), 2.54 (sept, $^3J = 6.8$, 1H, Ar–C*H*$(CH_3)_2$), 2.01 (m, 1H, Os–CH_2–), 1.94 (s, 3H, Ar–CH_3), 1.61 (m, 1H, Os–CH_2–), 1.62 ($^2J(^{31}P,^1H) = 9.5$, 9H, $P(Me_3)$), 1.14 (t, $^3J = 6.8$ 3H, Os–CH_2–CH_3), 1.02 (d, $^3J = 6.9$, 3H, Ar–CH(C$H_3)_2$), 0.95 (d, $^3J = 6.8$, 3H, Ar–CH(C$H_3)_2$). **^{13}C NMR** (CD_2Cl_2): δ 101.2 (s, C(1)), 89.8 (s, C(4)), 83.0 (d, Ar), 78.1 (d, Ar), 77.9 (d, Ar), 72.5 (d, Ar), 31.0 (d, Ar–*C*H$(CH_3)_2$), 26.1 (q, Os–CH_2–*C*H_3), 20.4 (qd, $^1J(^{31}P,^{13}C) = 28.3$, $P(CH_3)_3$), 18.2, 17.7 (q, Ar–CH(*C*$H_3)_2$), 17.6 (q, Ar–*C*H_3), −10.5 (td, $^2J(^{31}P,^{13}C) = 11.6$, Os–$CH_2$–). **^{31}P NMR** ($CD_2Cl_2$): δ −50.8. **^{187}Os NMR** ($CDCl_3$): δ −3605 (d, $^1J(^{187}Os,^{31}P) = 288$).

4.6.2. (p-Cymene)OsI(Me)P^{i}Pr$_3$ (6c) and (p-cymene)Os(Me)$_2$P^{i}Pr$_3$ (7c)

Under a nitrogen atmosphere, a suspension of 10 mg (0.014 mmol) **1c** in 0.5 ml toluene was deep-frozen and a few drops (20 μl) of Al_2Me_6 (ca. 2 M in toluene) were added. The mixture was brought to thawing temperature and 0.5 ml acetone/H_2O (20:1) was added dropwise under constant stirring and cooling. Elution with Et_2O, vacuum-concentration and purification by column chromatography (neutral alox/Et_2O) gave a yellow fraction, which after drying in vacuum was identified by NMR spectroscopy as a mixture of **6c** and **7c** (1:1).

^{1}H NMR (toluene-d_8): δ 5.06 (d, $^3J = 5.2$, 1H, Ar, **6c**), 4.98 (d, $^3J = 5.8$, 1H, Ar, **6c**), 4.75 (d, $^3J = 5.7$, 1H, Ar, **6c**), 4.74 (d, $^3J = 5.9$, 1H, Ar, **6c**) 4.58 (d, $^3J = 5.5$, 2H, Ar, **7c**), 4.39 (d, $^3J = 5.5$, 2H, Ar, **7c**), 2.78 (sept, $^3J = 6.9$, 1H, Ar–C*H*$(CH_3)_2$, **6c**), 2.48–2.57 (m, 3H, P(C*H*$(CH_3)_2)_3$, **6c** and 1H, Ar–C*H*$(CH_3)_2$, **7c**), 2.35–2.25 (m, 3H, P(C*H*$(CH_3)_2)_3$, **7c**), 1.92 (s, 3H, Ar–CH_3, **6c**), 1.89 (s, 3H, Ar–CH_3, **7c**), 1.89 (d, $^3J(^{31}P,^1H) = 6.5$, 3H, OsCH_3, **6c**), 1.19 (d, $^3J = 6.8$, 6H, Ar–CH(C$H_3)_2$, **7c**), 1.13 (d, $^3J = 7.2$, 3H, Ar–CH(C$H_3)_2$, **6c**), 1.11 (d, $^3J = 7.2$, 3H, Ar–CH(C$H_3)_2$, **6c**), 1.03–1.10 (m, 36H, P(CH(C$H_3)_2)_3$, **6c** and **7c**), 0.83 (d, $^3J(^{31}P,^1H) = 5.9$, 6H, Os(C$H_3)_2$). **^{13}C NMR** (toluene-d_8): δ 104.1, 101.9 (s, C(1), **6c** + **7c**), 99.2 (2×) (s, C(4), **6c** + **7c**), 83.9 (d, Ar, **6c**), 79.3 (d, Ar, **6c**), 79.2 (d, 2× Ar, **7c**), 78.1 (d, 2× Ar, **7c**), 76.4 (d, Ar, **6c**), 76.2 (d, Ar, **6c**), 31.5 (d, Ar–*C*H$(CH_3)_2$, **6c**), 30.7 (d, Ar–*C*H$(CH_3)_2$, **7c**), 28.4 (dd, $^1J(^{31}P,^{13}C) = 28.4$, P(*C*H$(CH_3)_2)_3$, **7c**), 27.5 (dd, $^1J(^{31}P,^{13}C) = 27.3$, P(*C*H$(CH_3)_2)_3$, **6c**), 24.5, 23.6, 23.1, 21.8 (q, P(CH(*C*$H_3)_2)_3$, **7c** + **6c** and Ar–CH(*C*$H_3)_2$, **7c** + **6c**), 18.1, 17.9 (s, Ar–*C*H_3, **7c** + **6c**), −23.4 (qd, $^2J(^{31}P,^{13}C) = 12.9$, Os(*C*$H_3)_2$), −27.7 (qd, $^2J(^{31}P,^{13}C) = 13.0$, Os*C*$H_3$). **^{31}P NMR** (toluene-d_8): δ −2.4 (**7c**), −11.9 (**6c**).

4.6.3. Reaction of (p-cymene)OsI$_2$P^{i}Pr$_3$ (1c) with Al$_2$Me$_6$ in an NMR-tube at −45°C

Under a nitrogen atmosphere, 10 mg (0.014 mmol) **1c** were dissolved in toluene-d_8 in an NMR-tube. The solution was deep-frozen, a few drops of Al_2Me_6 in the same solvent were added and the tube was sealed under vacuum. Just before insertion into the NMR probe head, the mixture was brought to thawing temperature to facilitate shimming and tuning.

^{1}H NMR (toluene-d_8) (−45°C): δ 5.68 (b, 1H, Ar), 5.22 (b, 1H, Ar), 5.14 (b, 1H, Ar), 4.68 (b, 1H, Ar), 2.62–2.52 (m, 1H, Ar–C*H*(CH$_3$)$_2$), 1.95–2.11 (m, 3H, P(C*H*(CH$_3$)$_2$)$_3$), 1.88 (d, $^3J(^{31}P,^1H) = 6.3$, 3H, OsCH_3), 1.67 (s, 3H, Ar–CH_3) 1.14 (d, $^3J = 6.6$, 3H, Ar–CH(CH_3)$_2$), 0.98 (d, $^3J = 7.0$, 3H, Ar–CH(CH_3)$_2$), 0.85–0.76 (m, 18H, P(CH(CH_3)$_2$)$_3$). **^{31}P NMR** (toluene-d_8) (−45°C): δ −10.3.

4.6.4. (p-Cymene)OsI(Me)PCy$_3$ (6d)

Under a nitrogen atmosphere, 0.15 ml (0.25 mmol) Al_2Me_6 (ca. 2 M in toluene) were added dropwise at room temperature under constant stirring to a suspension of 20 mg (0.023 mmol) **1d** in 1.5 ml toluene. Work-up and purification were performed as described for **4a**, yielding 16 mg (0.021 mmol, 90%) of an orange-red solid.

^{1}H NMR ($CDCl_3$): δ 5.41 (d, $^3J = 5.5$, 1H, Ar), 5.24 (d, $^3J = 5.9$, 1H, Ar), 5.15 (d, $^3J = 5.9$, 1H, Ar), 5.10 (d, $^3J = 5.5$, 1H, Ar), 2.82 (sept, $^3J = 7.0$, 1H, Ar–C*H*(CH$_3$)$_2$), 2.39–2.28 (m, 3H, Cy, C(1)), 2.16 (s, 3H, Ar–CH_3), 2.11–1.63 (m, 15H, Cy), 1.61 (d, $^3J(^{31}P,^1H) = 6.6$, 3H, Os(CH_3)), 1.47–1.15 (m, 21H, Cy and Ar–CH(CH_3)$_2$). **^{31}P NMR** ($CDCl_3$): δ −22.8. **^{187}Os NMR** ($CDCl_3$): δ −3787 (d, $^1J(^{187}Os,^{31}P) = 273$).

4.6.5. Metallacycles

4.6.5.1. Synthesis of (p-cymene)OsMe{P(^{i}Pr)$_2$-CHMeCH$_2$} (8). Under an argon atmosphere, a suspension of 148 mg (0.2 mmol) **1c** in 2 ml toluene was cooled to 0°C. Via a syringe, 0.4 ml (0.8 mmol) Al_2Me_6 (ca. 2 M in toluene) were added slowly. Work-up and purification were performed as described for **4a**, yielding 41.5 mg (0.068 mmol, 34%) of a yellow-orange powder.

^{1}H NMR (CD_2Cl_2): δ 5.18 (d, $^3J = 5.3$, 1H, H(2)), 5.12 (d, $^3J = 5.3$, 1H, H(3)), 4.93 (d, $^3J = 5.9$, 1H, H(6)), 4.91 (d, $^3J = 5.5$, 1H, H(5)), 3.22 (qddd, 1H, $^2J(^{31}P,^1H) = 10.6$, $^3J = 7.3$, $^3J = 9.9$, $^3J = 11.0$, PC*H*(CH$_3$)(CH$_2$–)), 2.85 (dsept, $^2J(^{31}P,^1H) = 9.3$, $^3J = 7.5$, 1H, PC*H*(CH$_3$)$_2$), 2.66 (sept, $^3J = 7.0$, 1H, Ar–C*H*(CH$_3$)$_2$), 2.43 (dsept, $^2J(^{31}P,^1H) = 12.4$, $^3J = 7.0$, 1H, PC*H*(CH$_3$)$_2$), 2.26 (s, 3H, Ar–CH_3), 2.12 (ddd, $^2J = 9.0$, $^3J = 10.0$, $^3J(^{31}P,^1H) = 36.4$, 1H, –CH$_2$–, H^B), 1.62 (ddd, $^2J = 9.0$, $^3J = 10.8$, $^3J(^{31}P,^1H) = 4.6$, 1H, –CH$_2$–, H^A), 1.21–1.05 (m, 9H, P–CH(CH_3)$_2$), 1.18 (d, $^3J = 6.9$, 3H, Ar–CH(CH_3)$_2$), 1.09 (d, $^3J = 6.9$, 3H, Ar–CH(CH_3)$_2$), 0.96–0.87 (m, 6H, PCH(CH_3)$_2$). **^{13}C NMR** (CD_2Cl_2): δ 102.8 (s, C(1)), 92.8 (s, C(4)), 75.9 (d, C(5)), 75.5 (d, C(2)), 71.5 (d, C(3)), 71.0 (d, C(6)), 46.6 (dd, $^1J(^{31}P,^{13}C) = 36.2$, P*C*H(CH$_3$)CH$_2$–), 30.6 (d, Ar–*C*H(CH$_3$)$_2$), 28.2 (dd, $^1J(^{31}P,^{13}C) = 16.4$, P*C*H(CH$_3$)$_2$), 22.8 (q, Ar–CH(*C*H$_3$)$_2$), 22.8 (qd, $^2J(^{31}P,^{13}C) = 3.2$, PCH(*C*H$_3$)CH$_2$–), 22.3 (dd, $^1J(^{31}P,^{13}C) = 20.0$, P*C*H(CH$_3$)$_2$), 21.8 (q, Ar–CH(*C*H$_3$)$_2$), 19.4 (q, PCH(*C*H$_3$)$_2$), 19.2 (q, PCH(*C*H$_3$)$_2$), 19.1 (q, PCH(*C*H$_3$)$_2$), 17.9 (q, Ar–*C*H$_3$), 17.0 (qd, $^2J(^{31}P,^{13}C) = 4.2$, PCH(*C*H$_3$)$_2$), −12.8 (td, $^2J(^{31}P,^{13}C) = 34.4$, Os–*C*H$_2$CH(CH$_3$)P–). **^{31}P NMR** ($CD_2Cl_2$): δ −33.1. **^{187}Os NMR** (CD_2Cl_2): δ −3554 (d, $^1J(^{187}Os,^{31}P) = 210$).

4.6.5.2. (p-Cymene)OsMe{P(OPh)$_2$(OC$_6$H$_4$-o)} (13). Under a nitrogen atmosphere, 70 mg (0.1 mmol) (*p*-cymene)OsCl$_2$P(OPh)$_3$ in 2 ml toluene were cooled to −60°C. Under constant stirring, 0.2 ml Al_2Me_6 (0.33 mmol) (ca. 2 M in toluene) were added dropwise via a syringe into the reaction vessel. Work-up and purification were performed analogous to **4a**, yielding 60 mg (0.092 mmol, 92%) of a yellow oil.

^{1}H NMR ($CDCl_3$): δ 7.39 (dd, $^3J = 7.3$, $^4J = 1.5$, 1H, (OC$_6$H$_4$-*o*)), 7.21–7.29 (m, 6H, P(OPh)$_2$), 7.15–7.10 (m, 4H, P(OPh)$_2$), 6.95 (d, $^3J = 7.8$, 1H, (OC$_6$H$_4$-*o*)), 6.86 (dt, $^3J = 7.5$, $^4J = 1.2$, 1H, (OC$_6$H$_4$-*o*)), 6.68 (dt, $^3J = 7.2$, $^4J = 1.3$, 1H, (OC$_6$H$_4$-*o*)), 5.21 (d, $^3J = 5.9$, 1H, Ar), 5.06 (d, $^3J = 5.8$, 1H, Ar), 4.95 (d, $^3J = 5.7$, $^4J = 1.0$, 1H, Ar), 4.74 (d, $^3J = 5.8$, $^4J = 1.1$, 1H, Ar), 2.37 (sept, $^3J = 6.9$, 1H, Ar–C*H*(CH$_3$)$_2$), 1.96 (s, 3H, Ar–CH_3), 1.03 (d, $^3J = 6.9$, 3H, Ar–CH(CH_3)$_2$), 1.01 (d, $^3J = 6.9$, 3H, Ar–CH(CH_3)$_2$), 0.06 (d, $^3J(^{31}P,^1H) = 5.6$, 3H, OsCH_3). **^{13}C NMR** ($CDCl_3$): δ 160.2 (sd, $J = 19.4$, (OC$_6$H$_4$-*o*)), 152.4, 152.3 (s, C(1), P(OPh)$_2$), 141.7 (dd, $J = 2.4$, (OC$_6$H$_4$-*o*)), 137.9 (sd, $J = 12.3$, (OC$_6$H$_4$-*o*)), 129.5, 129.1 (d, C(3), C(5), P(OPh)$_2$), 123.9, 123.8 (d, C(4), P(OPh)$_2$), 122.5 (d, (OC$_6$H$_4$-*o*)), 122.1 (d, (OC$_6$H$_4$-*o*)), 120.8 (dd, $^3J = 5.3$, C(2), C(6), P(OPh)$_2$), 120.7 (dd, $^3J = 4.9$, C(2), C(6), P(OPh)$_2$), 110.0 (dd, $J = 14.6$, (OC$_6$H$_4$-*o*)), 105.2 (s, Ar, C(1)), 101.9 (s, Ar, C(4)), 85.4 (d, Ar), 84.7 (d, Ar), 83.3 (d, Ar), 81.9 (d, Ar), 30.7 (d, Ar–*C*H(CH$_3$)$_2$), 24.0, 22.6 (q, Ar–CH(*C*H$_3$)$_2$), 17.7 (q, Ar–*C*H$_3$), −28.8 (qd, $^2J(^{31}P,^{13}C) = 15.2$, Os*C*H$_3$). **^{31}P NMR** ($CDCl_3$): δ 119.1.

Acknowledgements

This work was supported by the Swiss National Science Foundation and by the Dr. Helmut Legerlotz-Stiftung.

References

[1] R.A. Sánchez-Delago, M. Rosales, M.A. Esteruelas, L.A. Oro, J. Mol. Catal. A 96 (1995) 231.
[2] H. Le Bozec, D. Touchard, P.H. Dixneuf, Adv. Organomet. Chem. 29 (1989) 163.
[3] A.G. Bell, W. Kozminski, A. Linden, W. von Philipsborn, Organometallics 15 (1996) 3124.
[4] E.J.M. Meier, W. Kozminski, A. Linden, P. Lustenberger, W. von Philipsborn, Organometallics 15 (1996) 2469.
[5] E.J.M. Meier, PhD Thesis, University of Zürich, 1996.
[6] J.A. Cabeza, P.M. Maitlis, J. Chem. Soc., Dalton Trans. (1985) 573.
[7] H. Werner, S. Stahl, W. Kohlmann, J. Organomet. Chem. 409 (1991) 285.
[8] W. Knaup, H. Werner, J. Organomet. Chem. 411 (1991) 471.
[9] J.A. Cabeza, B.E. Mann, P.M. Maitlis, C. Brevard, J. Chem. Soc., Dalton Trans. (1988) 629.
[10] J.A. Cabeza, A. Nutton, B.E. Mann, C. Brevard, P.M. Maitlis, Inorg. Chim. Acta 115 (1986) L47.
[11] J.A. Cabeza, B.E. Mann, C. Brevard, P.M. Maitlis, J. Chem. Soc., Chem. Comm. (1985) 65.
[12] R. Benn, H. Brenneke, E. Joussen, H. Lehmkuhl, F.L. Ortiz, Organometallics 9 (1990) 756.
[13] R. Benn, H. Brennecke, E. Joussen, H. Lehmkuhl, F.L. Ortiz, A. Rufinska, J. Am. Chem. Soc. 111 (1989) 8754.
[14] M.A. Gallop, B.F.G. Johnson, J. Lewis, J. Chem. Soc., Chem. Commun. (1987) 1831.
[15] A.A. Koridze, O.A. Kizas, N.M. Astakhova, P.V. Petrovskii, Y.K. Grishin, J. Chem. Soc., Chem. Commun. (1981) 853.
[16] R.I. Michelman, G.E. Ball, R.G. Bergman, R.A. Andersen, Organometallics 13 (1994) 869.
[17] H. Werner, K. Zenkert, J. Organomet. Chem. 345 (1988) 151.
[18] H. Werner, R. Werner, Chem. Ber. 115 (1982) 3766.
[19] H. Werner, K. Zenkert, J. Chem. Soc., Chem. Commun. (1985) 1607.
[20] M.A. Bennett, T.-N. Huang, J.L. Latten, J. Organomet. Chem. 272 (1984) 189.
[21] M.C.B. Colbert, S.L. Ingham, J. Lewis, N.J. Long, P.R. Raithby, J. Chem. Soc., Dalton Trans. (1994) 2215.
[22] A.A. Cherkas, N.J. Taylor, A.J. Carty, J. Chem. Soc., Chem. Commun. (1990) 385.
[23] J. Espuelas, M.A. Esteruelas, F.J. Lahoz, L.A. Oro, C. Valero, Organometallics 12 (1993) 663.
[24] M.A. Esteruelas, F.J. Lahoz, A.M. Lopez, E. Onate, L.A. Oro, Organometallics 14 (1995) 2496.
[25] C.K. Johnson, ORTEPII, Report ORNL-5138, Oak Ridge National Laboratory, Oak Ridge, TN, 1976.
[26] F.H. Allen, O. Kennard, Chem. Design Autom. News 8 (1993) 31.
[27] C.A. Tolman, Chem. Rev. 77 (1977) 313.
[28] T. Bartik, T. Himmler, H.-G. Schulte, K. Seevogel, J. Organomet. Chem. 272 (1984) 29.
[29] D.B. Pourreau, G.L. Geoffroy, A.L. Rheingold, S.J. Geib, Organometallics 5 (1986) 1337.
[30] Y. Kawano, H. Tobita, H. Ogino, Organometallics 13 (1994) 3849.
[31] E.J.M. Meier, W. Kozminski, W. von Philipsborn, Magn. Reson. Chem. 34 (1996) 89.
[32] C.J. Jameson, in: J. Mason (Ed.), Multinuclear NMR, Plenum, New York, 1987, p. 89.
[33] N. Juranic, Coord. Chem. Rev. 96 (1989) 253.
[34] R.W. Kunz, Helv. Chim. Acta 63 (1980) 2054.
[35] D. Nanz, A. Bell, W. Kozminski, E.J. Meier, V. Tedesco, W. von Philipsborn, BRUKER Rep. 143 (1996) 29.
[36] A.C.T. North, D.C. Phillips, F.S. Mathews, Acta Crystallogr. Sect. A 24 (1968) 351.
[37] P.T. Beurskens, G. Admiraal, G. Beurskens, W.P. Bosman, S. García-Granda, J.M.M. Smits, C. Smykalla, Dirdif-92, the DIRDIF program system, Technical Report of the Crystallography Laboratory, University of Nijmegen, The Netherlands, 1992.
[38] G.M. Sheldrick, Shelxs-86, Acta Crystallogr. Sect. A 46 (1990) 467.
[39] Texsan, Single Crystal Structure Analysis Software, Version 5.0., Molecular Structure. The Woodlands, TX, 1989.
[40] H.D. Flack, Acta Crystallogr. Sect. A 39 (1983) 876.
[41] G. Bernardinelli, H.D. Flack, Acta Crystallogr. Sect. A 41 (1985) 500.
[42] D.J. Watkin, J.R. Carruthers, P.W. Betteridge, Crystals User Guide, Chemical Crystallography Laboratory, Oxford, UK, 1985.
[43] E.N. Maslen, A.G. Fox, M.A. O'Keefe, Table 6.1.1.1, in: A.J.C. Wilson (Ed.), International Tables for Crystallography, Vol. C, Kluwer Academic, Dordrecht, 1992, pp. 477–486.
[44] R.F. Stewart, E.R. Davidson, W.T. Simpson, J. Chem. Phys. 42 (1965) 3175.
[45] J.A. Ibers, W.C. Hamilton, Acta Crystallogr. 17 (1964) 781.
[46] D.C. Creagh, W.J. McAuley, Table 4.2.6.8, in: A.J.C. Wilson (Ed.), International Tables for Crystallography, Vol. C, Kluwer Academic, Dordrecht, 1992, pp. 219–222.